International Journal of Thermophysics, Vol. 12, No. 6, 1991

Thermal Conductivity of Gaseous HFC-134a, HFC-143a, HCFC-141b, and HCFC-142b

Y. Tanaka,[1] M. Nakata,[1] and T. Makita[1]

Received March 7, 1991

The thermal conductivity of new environmentally acceptable fluorocarbons HFC-134a (CH_2FCF_3), HFC-143a (CH_3CF_3), HCFC-141b (CH_3CCl_2F), and HCFC-142b (CH_3CCl_2F) in the gaseous phase has been measured in the temperature range 293–353 K at pressures up to 4 MPa. The thermal conductivity has been measured with a coaxial-cylinder cell on a relative basis. The apparatus was calibrated with He, Ne, Ar, Kr, N_2, CH_4, and SF_6 as reference fluids. The uncertainty of the experimental data obtained is estimated to be within 2% except for the uncertainty associated with the reference thermal-conductivity values. The excess thermal conductivity has been correlated satisfactorily as a function of density.

KEY WORDS: coaxial-cylinder method; fluorocarbons; halogenated ethane; R134a; R143a; R141b; R142b; refrigerants; thermal conductivity.

1. INTRODUCTION

To evaluate the performance of possible alternatives to the fully halogenated chlorofluorocarbons as working fluids in refrigeration or heat-pumping applications, an accurate knowledge of the thermophysical properties over wide ranges of temperature and pressure is required. The thermal conductivity of the refrigerants has a very important role in the design of heat exchangers. However, reliable information for the thermal conductivity of promising alternatives, especially at high pressures, is scarce. Even if available, there exist considerable discrepancies among the literature values obtained by different investigators. Hence, there is an urgent need for an accurate and systematic measurements of the thermal conductivity and for a critical evaluation of the data in the literature.

[1] Department of Chemical Engineering, Kobe University, Kobe 657, Japan.

840/12/6-1

The present investigation was undertaken to obtain accurate thermal-conductivity data of new environmentally acceptable alternatives to fully halogenated CFCs, namely, HFC-134a (1,1,1,2-tetrafluoroethane), HFC-143a (1,1,1-trifluoroethane), HCFC-141b (1,1-dichloro-1-fluoroethane), and HCFC-142b (1-chloro-1,1-difluoroethane) in the gaseous phase at temperatures from 293 to 353 K and pressures up to 4 MPa.

2. EXPERIMENTAL

2.1. Thermal-Conductivity Cell

The thermal conductivity was measured with a coaxial-cylinder cell. A cross-sectional view of the cell is shown in Fig. 1. The apparatus consists of three concentric copper cylinders (a, b, and c) fixed vertically in a brass high-pressure vessel (d). A heater (e) is located in the inner cylinder (a). The heater is made of constantan wire wound on a threaded phenol resin. The central 70 mm of the heater was used as a main heater. The remainder, 70 mm at both ends, was used as guard heaters to minimize axial heat loss and to keep the thermal field uniform near the ends of the main heater. The sample fluid is restricted in the annular gap (g) of 0.5 mm between the emitter (b) and the receiver (c) by means of four O-rings (j). The fluid is isolated completely from the heater (e) and other electric parts contained in the inner cylinder. This structure differs from that which has been employed for gases in our earlier studies [1–3]. Stainless-steel spacers (f), whose contact length with the receiver (c) is 1 mm, are welded on both ends of the emitter (b). To minimize axial heat loss, thermal insulaters (h) are provided on both ends of the emitter. The temperature difference across the fluid layer was measured with four sets of copper–constantan differential thermocouples (i) installed in the emitter and the receiver. Two sets are installed at the center of the main heater to measure the temperature difference, and others are installed near the guard heaters to confirm the uniformity of the thermal field. The temperature difference was measured with a digital nanovoltmeter to within ± 10 nV. The high-pressure vessel was placed vertically in a liquid thermostat controlled to within ± 10 mK. The pressure was measured with a digital pressure gauge with an uncertainty of 1 kPa.

2.2. Calibration of the Cell

The total electrical energy dissipated in the main heater, Q, provides both the radial heat flux required to maintain a constant temperature gradient ΔT of 0.50 K across the fluid layer, and a small amount of axial

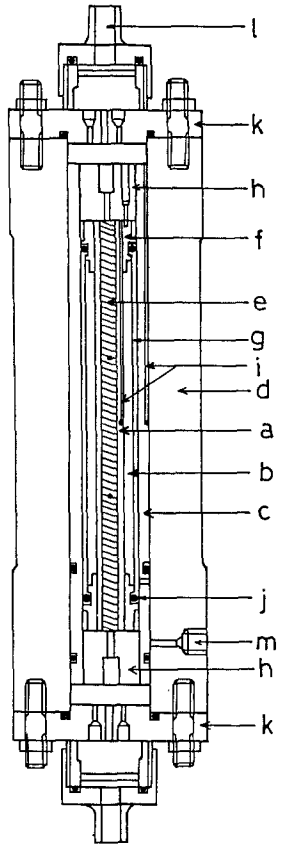

Fig. 1. Cross-sectional view of the thermal conductivity cell. (a) Inner cylinder (copper; o.d. = 14 mm, l = 210 mm). (b) Emitter (copper; o.d. = 27 mm, l = 210 mm). (c) Receiver (copper; o.d. = 40 mm, i.d. = 28 mm, l = 270 mm). (d) High-pressure vessel (brass; o.d. = 98 mm, i.d. = 40 mm, l = 300 mm). (e) Heater (o.d. = 8 mm, l = 210 mm). (f) Spacer (stainless steel). (g) Sample layer (o.d. = 28 mm, i.d. = 27 mm). (h) Thermal insulator (phenol resin). (i) Thermocouple (copper–constantan). (j) O-ring. (k) Flange (brass). (l) Opening for electric leads. (m) Sample inlet.

heat loss through spacers, insulators, and electrical leads. Therefore, the axial heat loss should be corrected empirically by calibration with reference fluids with known thermal conductivities. The following relation should hold if the temperature difference is kept constant throughout the experimental runs:

$$\frac{Q}{\Delta T}=\frac{1}{C_1+C_2/\lambda}+C_3 \tag{1}$$

where C_1, C_2, and C_3 are cell constants. To calibrate the cell, the quantity $Q/\Delta T$ was measured for each isotherm using helium, neon, argon, krypton, nitrogen, methane, and sulfur hexafluoride. These fluids were selected because of the availability of reliable reference data for λ. The reference values include seven data points at 0.1 MPa and two at 5 MPa (N_2 and Ar) for each isotherm. From the reference values of these gases [4–8] the cell constants were determined at each temperature by least-squares fits. Typical calibration curves obtained at 293 and 353 K are shown in Fig. 2. This calibration procedure enabled us to determine the thermal conductivity with a maximum uncertainty less than 0.8%. The actual calibration range is indicated by solid lines.

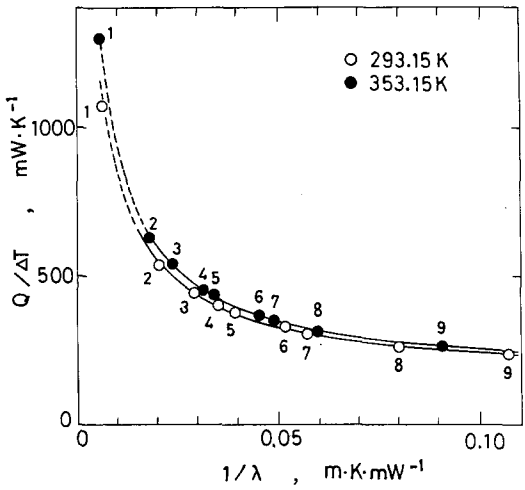

Fig. 2. Calibration curve for the coaxial-cylinder apparatus. (1) He, 0.1 MPa; (2) Ne, 0.1 MPa; (3) CH_4, 0.1 MPa; (4) N_2, 5 MPa; (5) N_2, 0.1 MPa; (6) Ar, 5 MPa; (7) Ar, 0.1 MPa; (8) SF_6, 0.1 MPa; (9) Kr, 0.1 MPa.

Table I. Sources of Error and Their Contribution to Thermal Conductivity

Error source	Uncertainty in measurement	Uncertainty contributing to λ (%)
Temperature	50 mK	0.1
Temperature difference	1 mK	0.5
Pressure	5 kPa	0.1
Power input	0.15%	0.3
Calibration of the cell	1%	1.0

2.3. Sample Fluids

The sample fluids, HFC-134a, HFC-143a, HCFC-141b, and HCFC-142b, were synthesized and purified by Daikin Industries, Ltd., with purities better than 99.9%. The reference gases were obtained from commercial sources with a specification of minimum purity of 99.99% except methane and sulfur hexafluoride, whose purities were better than 99.5%. These fluids were used without further purification.

2.4. Experimental Uncertainty

The thermal conductivity values obtained are affected by several sources of experimental error. The major sources of error and their estimated contribution are listed in Table I. Convection can be neglected if the Rayleigh number is less than 1000 for a vertical coaxial-cylinder apparatus [9]. The influence of convection was found to be negligible throughout the present experimental conditions. The influence of thermal radiation across the sample layer is also small and within the experimental error. The effect of pressure and temperature on the dimensions of the apparatus should be small, and it is taken into account by the above calibration. Based on the above discussion of error sources and reproducibility of the measurements, the maximum uncertainty in the experimental data is estimated to be less than 2% except the uncertainty accompained with the standard values of reference fluids.[2]

3. RESULTS

The experimental results for HFC-134a, HFC-143a, HCFC-141b, and HCFC-142b are presented in Tables II to V, respectively, as functions of

[2] The uncertainty of the standard values is estimated to be within 2–4%.

Table II. Thermal Conductivity of Gaseous HFC-134a
[P, Pressure (MPa); λ, Thermal Conductivity ($mW \cdot m^{-1} \cdot K^{-1}$)]

293.15 K		313.15 K		333.15 K		353.15 K	
P	λ	P	λ	P	λ	P	λ
0.10	12.3	0.10	14.1	0.10	15.6	0.10	17.8
0.20	12.5	0.20	14.3	0.20	15.7	0.29	17.8
0.30	12.6	0.30	14.4	0.40	15.9	0.48	18.4
0.40	13.0	0.40	14.4	0.60	16.1	0.80	18.7
0.50	13.2	0.50	14.6	0.80	16.5	1.26	19.5
0.55	13.5	0.60	14.8	1.00	16.8	1.59	20.3
		0.70	14.9	1.25	17.4	1.95	21.6
		0.80	15.2	1.44	18.1	2.22	23.3
		0.90	15.6	1.63	18.6	2.54	25.6

Table III. Thermal Conductivity of Gaseous HFC-143a
[P, Pressure (MPa); λ, Thermal Conductivity ($mW \cdot m^{-1} \cdot K^{-1}$)]

293.15 K		313.15 K		333.15 K		353.15 K	
P	λ	P	λ	P	λ	P	λ
0.11	12.6	0.11	13.8	0.11	14.9	0.10	16.8
0.29	12.9	0.27	13.9	0.25	15.0	0.50	17.4
0.50	13.1	0.51	14.5	0.50	15.2	1.08	18.3
0.74	13.6	0.77	14.8	1.00	15.9	1.49	18.9
0.99	14.2	1.01	15.2	1.48	17.0	2.10	20.1
		1.25	15.6	2.00	18.3	2.88	23.1
		1.51	16.3	2.50	21.1	3.30	25.2
						3.60	28.2
						3.77	31.2
						3.89	33.6
						3.98	37.5

Table IV. Thermal Conductivity of Gaseous HCFC-141b
[P, Pressure (MPa); λ, Thermal Conductivity ($mW \cdot m^{-1} \cdot K^{-1}$)]

T (K)	P	λ
293.15	0.1	8.2
313.15	0.1	9.5
333.15	0.1	10.7
353.15	0.1	12.1

Table V. Thermal Conductivity of Gaseous HCFC-142b
[P, Pressure (MPa); λ, Thermal Conductivity ($mW \cdot m^{-1} \cdot K^{-1}$)]

293.15 K		313.15 K		333.15 K		353.15 K	
P	λ	P	λ	P	λ	P	λ
0.10	10.9	0.10	12.1	0.11	13.3	0.11	14.2
0.20	11.1	0.20	12.3	0.20	13.3	0.29	14.3
0.26	11.3	0.30	12.3	0.31	13.4	0.57	14.5
		0.40	12.5	0.40	13.5	0.85	15.0
		0.50	12.9	0.51	13.7	1.17	15.7
				0.64	13.8	1.35	16.5
				0.82	14.4		

temperature and pressure. Each table contains the thermal conductivity at nominal temperatures. The thermostat was maintained constant at a temperature 0.25 K lower than the nominal temperature, since the temperature difference ΔT across the sample layer was fixed to 0.50 K in the present work.

3.1. Thermal Conductivity at Atmospheric Pressure

The thermal conductivities of gaseous HFCs and HCFCs measured at atmospheric pressure are plotted in Fig. 3 together with the recommended values for CFC-11 [10] and CFC-12 [11]. The thermal conductivity of each fluorocarbon increases almost linearly with increasing temperature. HFC-134a and HCFC-141b are promising candidates as alternatives to CFC-12 and CFC-11, respectively. The thermal conductivity of each alternative is higher than that of the corresponding CFC. In Fig. 4, the temperature dependence of the thermal conductivity of HFC-134a is plotted together with some literature values [12–14]. The present results are about 9% lower than the zero-density data of Richard and Shankland [12, 13] measured by the transient hot-wire method, and about 5% lower than those cited in the ICI technical report [14]. However, the temperature coefficient of λ, $(\partial\lambda/\partial T)_p$, is in good agreement with the literature values. Concerning HCFC-142b as shown in Fig. 5, the present results are more than 10% lower than the experimental data of Afshar and Saxena [15] obtained by the thermal-conductivity column method. The present measurements may be more reliable than their results, because the thermal-conductivity column method is suitable for measurements at higher temperatures up to 1500 K, and Afshar and Saxena [15] reported that the accuracy of measurements was $\pm 5.6\%$ at 297 K.

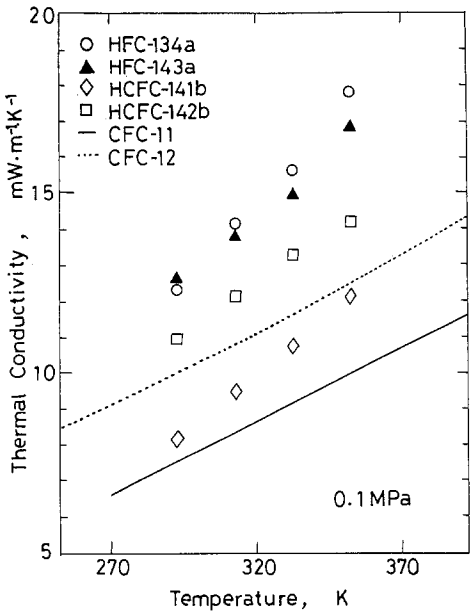

Fig. 3. Comparison of thermal conductivities of fluorocarbons studied at atmospheric pressure.

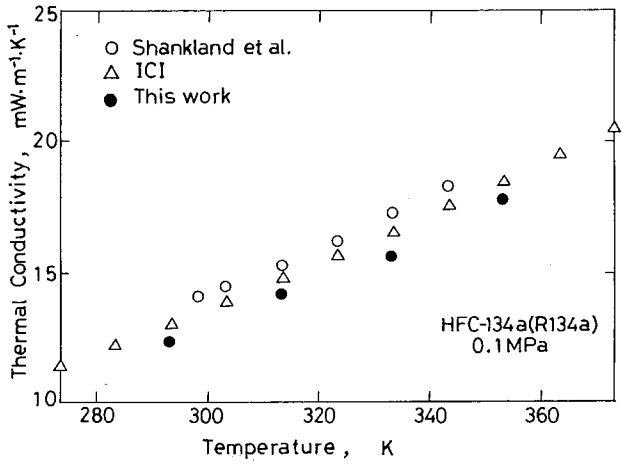

Fig. 4. Thermal conductivity of HFC-134a at atmospheric pressure.

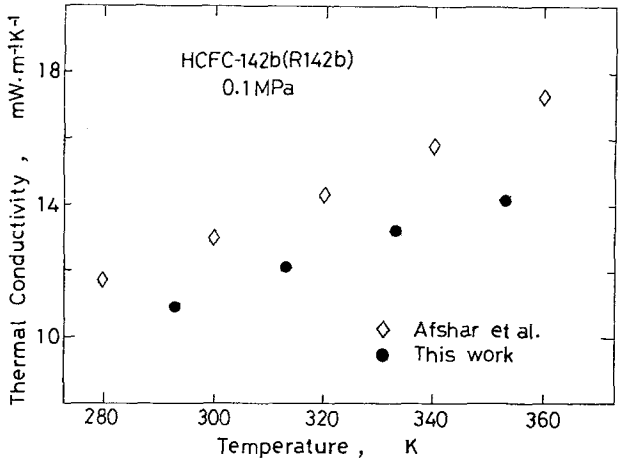

Fig. 5. Thermal conductivity of HCFC-142b at atmospheric pressure.

3.2. Thermal Conductivity at High Pressure

The pressure dependence of the thermal conductivity of gaseous HFC-134a, HFC-143a, and HCFC-142b is shown in Figs. 6–8. The thermal conductivity increases monotonously with increasing pressure. Each

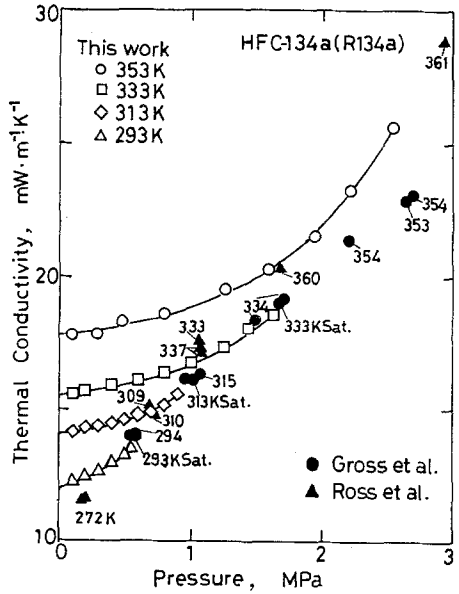

Fig. 6. Isothermal pressure dependences of thermal conductivity of HFC-134a.

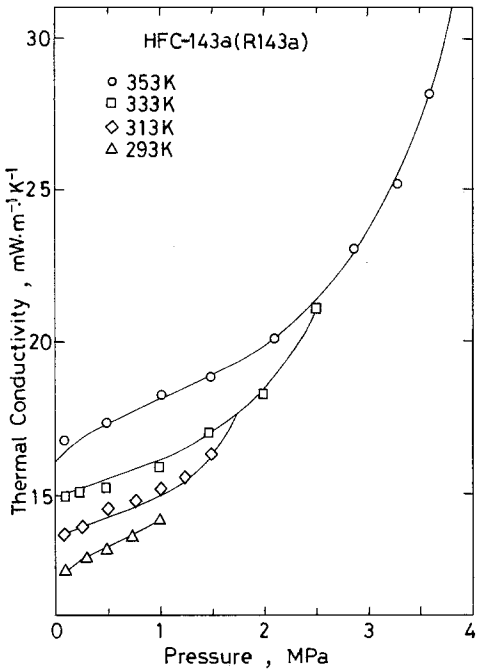

Fig. 7. Isothermal pressure dependences of thermal conductivity of HFC-143a.

isotherm is discontinuous at the saturation pressure except the isotherm of HFC-143a at 353 K, which is the only supercritical isotherm in the present work. The apparent thermal conductivity increases abruptly at the saturation pressure with increasing amounts of saturated liquid coexisting with vapor and, finally, reaches the thermal conductivity of saturated liquid.

The pressure coefficient of the thermal conductivity, $(\partial\lambda/\partial P)_T$, is always positive and increases with increasing pressure. The temperature coefficient $(\partial\lambda/\partial T)_p$ is also positive in the present experimental range. In Fig. 6, the experimental data of Ross et al. [16] and Gross et al. [17] measured by the transient hot-wire method for HFC-134a in the vapor phase near the saturation line are plotted together with our data for a comparison. These three sets of data are found to be in satisfactory agreement near the saturation line except for several data points of Gross et al. [17] at 354 K, although a strict comparison of the data is impossible.

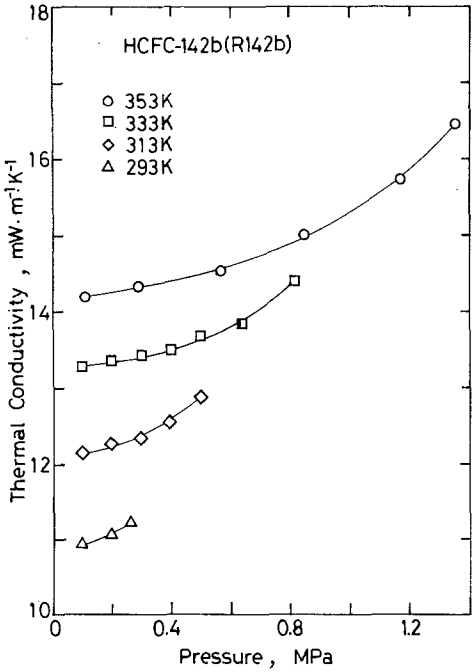

Fig. 8. Isothermal pressure dependences of thermal conductivity of HCFC-142b.

4. DISCUSSION

4.1. Empirical Correlation with Temperature and Pressure

For practical use, the thermal conductivity obtained has been correlated with temperature and pressure by a simple polynomial:

$$\lambda = a_0 + a_1 P + a_2 P^2 + a_3 P^3 \tag{2}$$

where

$$a_0 = a_{00} + a_{01} T$$
$$a_1 = a_{10} + a_{11} T + a_{12} T^2$$
$$a_2 = a_{20} + a_{21} T + a_{22} T^2$$
$$a_3 = a_{30} + a_{31} T + a_{32} T^2$$

λ is the thermal conductivity in $\mathrm{mW \cdot m^{-1} \cdot K^{-1}}$, P is the pressure in MPa, and a_{ij} ($i = 0$–3, $j = 0$–2) are empirical coefficients. The numerical values of

Table VI. Empirical Coefficients in Eq. (2) (λ in $mW \cdot m^{-1} \cdot K^{-1} \cdot K^{-1}$, T in K, and P in MPa)

Fluorocarbon	HFC-134a	HFC-143a	HCFC-142b
Coefficient			
a_{00}	-1.339×10	-7.920	-2.529×10
a_{01}	8.72932×10^{-2}	6.83523×10^{-2}	1.78991×10^{-1}
a_{02}	—	—	-1.89651×10^{-4}
a_{10}	1.14571×10^{2}	1.41237×10^{2}	2.28778×10
a_{11}	-7.15448×10^{-1}	-8.50684×10^{-1}	-1.37595×10^{-1}
a_{12}	1.12416×10^{-3}	1.29854×10^{-3}	2.03532×10^{-4}
a_{20}	-3.61873×10	-1.14883×10^{2}	8.72296×10
a_{21}	2.44739×10^{-1}	6.66038×10^{-1}	-4.65880×10^{-1}
a_{22}	-4.12885×10^{-4}	-9.75090×10^{-4}	6.31111×10^{-4}
a_{30}	1.11450×10^{2}	6.57458×10	—
a_{31}	-6.49243×10^{-1}	-3.71923×10^{-1}	—
a_{32}	9.50136×10^{-4}	5.29149×10^{-4}	—
Mean dev. (%)	0.53	0.93	0.25
Max. dev. (%)	1.15	2.73	0.55

the coefficients were determined by least-squares fitting and are listed in Table VI together with the mean and the maximum deviations of the experimental data from Eq. (2). The solid lines in Figs. 6, 7, and 8 are values calculated by Eq. (2). Except for two isotherms at 313.15 and 333.15 K of HCFC-143a, Eq. (2) is found to correlate the present experimental results with temperature and pressure satisfactorily.

4.2. Correlation by Means of Excess Thermal Conductivity

Most correlations describing the effect of pressure on the thermal conductivity have used the simple correlating technique based on the excess thermal conductivity concept. In this scheme, the excess thermal conductivity, $\lambda - \lambda_0$, is expressed as a function of density or reduced density as follows:

$$\lambda - \lambda_0 = f(\rho) \tag{3}$$

where λ_0 is the thermal conductivity at atmospheric pressure. Temperature and pressure do not enter explicitly in the equation, but their effects are included in the parameters λ_0 and ρ. The excess thermal conductivity of HFC-134a is plotted against density in Fig. 9. The excess thermal

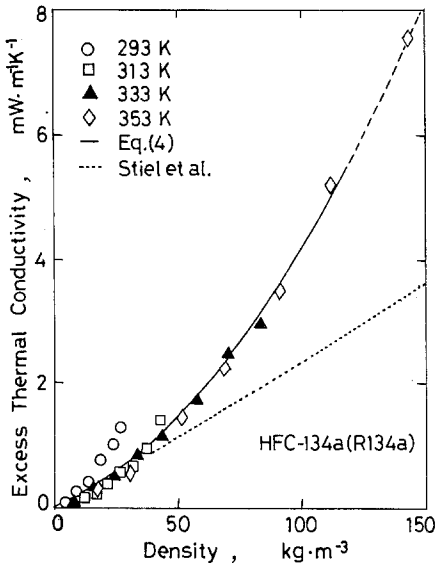

Fig. 9. Excess thermal conductivity of HFC-134a as a function of density.

conductivity at all temperatures can be expressed approximately as a single function of density except the isotherm at 293.15 K. The experimental data obtained can be correlated by

$$\lambda - \lambda_0 = b_1\rho + b_2\rho^2 \tag{4}$$

where λ and λ_0 are measured in $\mathrm{mW \cdot m^{-1} \cdot K^{-1}}$ and ρ in $\mathrm{kg \cdot m^{-3}}$. The density was calculated from the equations of state [18, 19]. The solid line in Fig. 9 represents the above equation. The empirical coefficients b_1 and b_2 are given in Table VII together with the mean and the maximum deviations of the thermal conductivity from Eq. (4).

Stiel and Thodos [20] presented a generalized correlation by assuming that $f(\rho)$ depends only on T_c, P_c, V_c, M, and ρ. By dimensional

Table VII. Empirical Coefficients in Eq. (4)

Refrigerant	$b_1 \times 10^2$	$b_2 \times 10^4$	Mean dev. (%)	Max. dev. (%)
HFC-134a	1.728	2.461	0.91	4.70
HFC-143a	1.941	2.938	1.48	3.17
HCFC-142b	0.9610	4.160	0.60	2.11

analysis, they obtained the following equation for nonpolar substances including inert gases, diatomic gases, CO_2, and hydrocarbons.

$$(\lambda - \lambda_0)\,\zeta Z_c^5 = 14.0 \times 10^{-8} \exp[(0.535\,\rho_r) - 1], \qquad \rho_r < 0.5 \tag{5}$$

where ζ is the thermal conductivity parameter defined as $T_c^{1/6} M^{1/2} / P_c^{2/3}$, Z_c the compressibility factor at the critical point, and ρ_r the reduced density. An attempt was made to use this equation to predict the excess thermal conductivity of refrigerants studied in this work. The predicted values are shown in Fig. 9 by the dotted line. It was found that the equation was able to predict the excess thermal conductivity of refrigerants studied only in a quite low density region, $\rho_r < 0.07$. The equation should not be suitable to estimate high-pressure thermal conductivity of polar substances such as NH_3, H_2O, and refrigerants.

5. CONCLUSION

As a continuation of the study of the thermophysical properties of stratospherically safe alternatives to fully halogenated chlorofluorocarbons, we have measured the thermal conductivity of gaseous HFC-134a, HFC-143a, HCFC-141b, and HCFC-142b at temperatures from 293 to 353 K under pressures up to 4 MPa or saturation pressure using a stationary coaxial-cylinder thermal conductivity apparatus. Recently the traditional stationary method for measuring thermal conductivity has been replaced almost completely by the transient hot-wire technique owing to the rapid progress in electronics and microcomputer technology. The transient hot-wire method has gained acceptance as one of the most reliable and accurate methods of thermal conductivity measurements of gases and liquids. According to Ross et al. [16], however, this method is not always suitable for the measurements with the refrigerants in the dilute gas phase and in the critical region. In the gas phase the vapor pressures of the refrigerants are often sufficiently low that the current theory of the transient hot-wire technique becomes inapplicable. Considering this situation, the authors hope that the stationary method, inclulding the parallel-plate apparatus, may play a complementary role in the thermal conductivity measurements of fluids until the difficulties encountered in the transient hot-wire method are overcome. It is very important for us that several kinds of experimental data obtained by quite different methods based on a variety of measuring principles are consistent with each other within the mutual uncertainties. The authors also hope that the present experimental results may contribute to the selection of alternatives to the fully halogenated chlorofluorocarbon refrigerants.

ACKNOWLEDGMENTS

The authors would like to express their sincere appreciation to Daikin Industries, Ltd., for the special synthesis and careful purifications of the sample fluids. The financial support for this work was provided in part by a Grant-in-Aid for Scientific Research from the Ministry of Education, Japan.

REFERENCES

1. Y. Tanaka, M. Noguchi, H. Kubota, and T. Makita, *J. Chem. Eng. Jpn.* **12**:171 (1979).
2. T. Makita, Y. Tanaka, Y. Morimoto, M. Noguchi, and H. Kubota, *Int. J. Thermophys.* **2**:249 (1981).
3. Y. Tanaka, H. Ueno, H. Kubota, and T. Makita, *Trans . JAR* **5**:61 (1988).
4. J. Kestin, K. Knierim, E. A. Mason, B. Najafi, S. T. Ro, and M. Waldman, *J. Phys. Chem. Ref. Data* **13**:229 (1984).
5. B. A. Younglove and H. J. M. Hanley, *J. Phys. Chem. Ref. Data* **15**:1323 (1986).
6. H. J. M. Hanley, R. D. McCarty, and W. M. Haynes, *J. Phys. Chem. Ref. Data* **3**:979 (1974).
7. H. J. M. Hanley, W. M. Haynes, and R. D. McCarty, *J. Phys. Chem. Ref. Data* **6**:597 (1977).
8. V. V. Burinskii, E. E. Totskii, and T. V. Yankova, *Teplofiz. Vys. Temp.* **25**:401 (1987).
9. H. Kraussold, *Forsch. Geb. Ing. Wes.* **5**:186 (1934).
10. American Society of Heating, Refrigerating and Air-Conditioning Engineers, (eds.), *Thermophysical Properties of Refrigerants* (ASHRAE Inc., New York, 1973).
11. Japanese Association of Refrigeration (eds.), *Thermophysical Properties of Refrigerants (R12, Dichlorodifluoromethane)* (JAR, Tokyo, 1981).
12. I. R. Shankland, R. S. Basu, and D. P. Wilson, *Proceedings of the IIR Conference, Commissions B1, B2, E1, and E2* (Purdue University, West Lafayette, Ind., 1988), pp. 305–311.
13. R. G. Richard and I. R. Shankland, *Int. J. Thermophys.* **10**:673 (1989).
14. ICI Chemicals and Polymers Ltd. (ed.), *"Arcton" 134a Preliminary Data Sheet* (ICI Chemicals & Polymers Ltd., The Heath, Runchor, Cheshire, England, 1988).
15. R. Afshar and S. C. Saxena, *Int. J. Thermophys.* **1**:51 (1980).
16. M. Ross, J. P. M. Trusler, W. A. Wakeham, and M. Zalaf, *Proceedings of IIR Commission B1 Meeting*, Herzlia, Israel (1990), pp. 89–94.
17. U. Gross, Y. W. Song, J. Kallweit, and E. Hahne, *Proceedings of IIR Commission B1 Meeting*, Herzlia, Israel (1990), pp. 103–108.
18. H. Sato and K. Watanabe, Private communication.
19. W. H. Mears, R. F. Stahl, S. R. Orfeo, R. C. Shair, L. F. Kells, W. Thompson, and H. McCann, *Ind. Eng. Chem.* **47**:1449 (1955).
20. L. I. Stiel and G. Thodos, *AIChE J.* **10**:26 (1964).